

# ENHANCEMENT OF THE EFFICIENCY OF ACOUSTO-OPTIC DIFFRACTION DUE TO THE ELLIPTICITY OF EIGEN OPTICAL WAVES, CAUSED BY THE ELECTRO-GYRATION EFFECT IN LEAD GERMANATE CRYSTALS

O. MYS, D. ADAMENKO, R. VLOKH

O.G. Vlokh Institute of Physical Optics, 23 Dragomanov Str., 79005, Lviv, Ukraine,  
e-mail: vlokh@ifp.lviv.ua

Received: 15.02.2024

**Abstract.** It has been shown for the first time that the electric field can enhance the acousto-optic (AO) figure of merit due to the induced ellipticity of eigenwaves through the electro-gyration effect. As a result of the analysis, we have revealed that for the isotropic types of interaction, the increasing of the strength of the electric field results in the broadening of the full width at half maximum (FWHM) of the peak of the AO figure of merit, while almost does not affect the maximal value of this peak. The FWHM of the peak of the AO figure of merit tends to saturation with increasing electric field strength. For anisotropic types of diffraction, the peak of the AO figure of merit is not observed, but with increasing the electric field strength, the surface of the AO figure of merit is expanded.

**Keywords:** acousto-optic diffraction, acousto-optic figure of merit, effective elasto-optic coefficient, electro-gyration, optical activity, ellipticity of eigen optical waves

**UDC:** 535.4, 534.2

**DOI:** 10.3116/16091833/Ukr.J.Phys.Opt.2024.03001

## 1. Introduction

The efficiency of acousto-optic (AO) Bragg diffraction ( $\eta = I_d / I_0$ ) is one of the main parameters in the acousto-optics that determines the portion of the light intensity ( $I_d$ ) which is transferred to the diffraction maximum in relation to the intensity of the incident wave ( $I_0$ ). In the case of  $\eta \ll 1$ , the efficiency of AO diffraction is determined by the relation:

$$\eta = M_2 \frac{\pi^2 L}{2\lambda_0^2 H \cos^2 \theta_B} P_{ac}, \quad (1)$$

where  $L$  – is the interaction length,  $H$  – is the height of the acoustic beam,  $\theta_B$  – is the Bragg angle,  $\lambda_0$  – is the wavelength of optical radiation in the vacuum and  $P_{ac}$  – is the acoustic wave (AW) power [1]. If not consider the set of geometrical parameters that are included in Eq. (1), the efficiency of AO diffraction is proportional to the AW power where the coefficient of proportionality is the AO figure of merit, which is determined as:

$$M_2 = \frac{n_i^3 n_d^3 p_{eff}^2}{\rho v^3}, \quad (2)$$

where  $n_i$  and  $n_d$  are the refractive indices of the incident and diffracted optical waves,  $p_{eff}$  – is the effective elasto-optic (EO) coefficient,  $v$  is the velocity of the AW, and  $\rho$  – is the material density. As one can see (Eq. (2)), the AO figure of merit depends on the constitutive

coefficient and AW velocity, which, in turn, depends on the elastic stiffness coefficients. Obviously, the lower the AW velocity, the higher the AO figure of merit. However, AW's low velocity causes AO devices' low repetition rate. Thus, the better way of enlarging of AO figure of merit is to increase the effective EO coefficient. The latter can be done by the optimization of the geometry of AO interaction (see e.g. [2-7]). However, the choice of the geometry of interaction with the maximum value of the AO figure of merit is mostly not optimal from the point of view of the phase-matching conditions and frequency of the AW, as well as the irrationality of crystallographic orientation.

In our recent works [8-10], it has been shown that an increase in the AO figure of merit can be achieved with the use of optically active crystals. At the same time, the polarization of the incident optical wave should be the same as the eigen elliptical (circular) polarization of the optical wave that propagates in the optically active crystal. This leads to the inclusion in the relation for the effective EO coefficient of the term that is proportional to the square of ellipticity of eigenwaves with the additional set of the components of the EO tensor. This causes the peak-like increase of the effective EO coefficient and AO figure of merit when the interacted optical waves propagate in the directions close to the optical axis where the ellipticity of the wave approaches unity. It has been found [11] that for such an aim, not only crystals that possess natural optical activity but also crystals in which optical activity of the Faraday type is induced by the magnetic field can be used. In such a case, the following questions appear: to reach the same aim, can the electric field-induced optical activity due to the electro-gyration effect be used, and what values of such a field are necessary? The solving of these problems is the goal of the present work.

## 2. Method of analysis

In the present work, we will consider the electro-gyration effect in the lead germanate crystals induced by spontaneous polarization that appears under proper ferroelectric phase transition. Then, the spontaneous polarization will be recalculated to the bias field using the formula:

$$E = \frac{P^s}{\varepsilon_0(\varepsilon_3 - 1)} \quad (3)$$

where  $\varepsilon_3$  is the dielectric permittivity along Z axis,  $\varepsilon_0 = 8.854 \times 10^{-12} \text{CV}^{-1}\text{m}^{-1}$  is the vacuum dielectric constant and  $P_3^s$  - spontaneous polarization.

$\text{Pb}_5\text{Ge}_3\text{O}_{11}$  crystals undergo a proper ferroelectric phase transition at 450 K with the symmetry change  $\bar{6}F3$  [12]. Lead germanate is optically active. The optical rotation occurring for the light propagation direction parallel to the optic axis is equal to  $\pm 5.58 \text{ deg/mm}$  at  $\lambda = 632.8 \text{ nm}$  [13]. The appropriate gyration tensor components are equal to  $g_{33} = \pm 4.16 \times 10^{-5}$  [12] and  $g_{11} = \pm 10.5 \times 10^{-5}$  at  $\lambda = 632.8 \text{ nm}$  [14], and the signs of the both tensor components are the same.

The gyration tensor components are proportional to the spontaneous polarization ( $P_3^s$ ):

$$g_{11} = \gamma_{113}P_3^s, \quad g_{33} = \gamma_{333}P_3^s \quad (4)$$

where  $\gamma_{113}$  and  $\gamma_{333}$  are the components of electro-gyration tensor defined in the units of reciprocal polarization and determined for the temperature close to the Curie point in the

paraelectric phase. The critical exponent of the temperature dependence of optical rotation and spontaneous polarization for lead germanate crystals is equal to  $0.39 \pm 0.01$  [15].

Switching of spontaneous electric polarization reverses the sign of optical activity. The single-domain lead germanate crystals can be either levorotary or dextrorotary, since their domains with the opposite signs of spontaneous polarization are enantiomorphous. In this work we choose a dextrorotary crystal (or “+” sign of spontaneous polarization). Then the extraordinary optical beam is right-handed while the ordinary beam is left-handed. The ordinary and extraordinary refractive indices for the lead germanate crystals are equal to  $n_o = 2.116$  and  $n_e = 2.151$  at the optical wavelength 632.8 nm [12], and the density of this material amounts to  $\rho = 7.33 \times 10^3 \text{ kg/m}^3$  [16].

Since we will simulate the optical activity induced by the electric field using spontaneous polarization, we have to carry out our analysis for the symmetry group of the paraelectric phase. Unfortunately, no data for EO coefficients for the temperature close to the phase transition in the paraelectric phase is available. However, one can use the EO coefficients determined for a multi-domain sample, which is associated with the point group of symmetry of the paraelectric phase since the spontaneous polarization is compensated in such a sample. The EO coefficients for the multidomain sample are as follows:  $p_{11} = 0.302 \pm 0.051$ ,  $p_{12} = 0.152 \pm 0.027$ ,  $p_{13} = 0.120 \pm 0.021$ ,  $p_{31} = 0.109 \pm 0.024$ ,  $p_{33} = 0.435 \pm 0.085$  [17]. The coefficient  $p_{66} = (p_{11} - p_{12}) / 2 = 0.150 \pm 0.078$ , while coefficients  $p_{44}$ ,  $p_{16}$ , and  $p_{45}$  are on one-two orders of magnitude smaller than the rest of the coefficients, and thus, one can neglect their values.

We will consider AO interaction in the  $XZ$  plane. The derivation of the equations for the effective EO coefficient for different types of AO interaction has been made similarly as in our recent works [9-11]. For the isotropic diffraction, it has been accepted that the diffraction angle is small enough ( $\gamma = 0.2 \text{ deg}$ ); thus, the Bragg angle is equal to  $\theta_B = 0.1 \text{ deg}$ . The ellipticity of the incident (the index ‘ $i$ ’) and diffracted (the index ‘ $d$ ’) optical eigenwaves are given by the relations [18]

$$\chi_i = \frac{1}{2G(\varphi_i)} \left( (n_o^2 - n_e'^2) - \sqrt{(n_o^2 - n_e'^2) + 4G(\varphi_i)^2} \right) \approx \frac{G(\varphi_i)}{n_o^2 - n_e'^2}, \quad (5)$$

$$\chi_d = \frac{1}{2G(\varphi_d)} \left( (n_o^2 - n_e'^2) - \sqrt{(n_o^2 - n_e'^2) + 4G(\varphi_d)^2} \right) \approx \frac{G(\varphi_d)}{n_o^2 - n_e'^2}, \quad (6)$$

where  $G$  is the scalar gyration parameter and  $\varphi_i$  and  $\varphi_d$  are the angles between the  $X$  axis and the propagation directions of the incident and diffracted optical waves, respectively. Note that the parameters involved in Eqs. (5) and (6) are given by

$$G(\varphi_i) = g_{33} \sin^2(\varphi_i) + g_{11} \cos^2(\varphi_i) \quad (7)$$

for the incident optical wave and

$$G(\varphi_d) = g_{33} \sin^2 \varphi_d + g_{11} \cos^2 \varphi_d \quad (8)$$

for the diffracted optical wave, with  $\varphi_d = \varphi_i + \gamma$  and  $\gamma$  being the angle of diffraction at the anisotropic interaction (Fig. 1). The corresponding refractive indices read as

$$n_e'^2(\varphi_i) = \frac{n_o^2 n_e^2}{n_o^2 \cos^2 \varphi_i + n_e^2 \sin^2 \varphi_i} \quad (9)$$

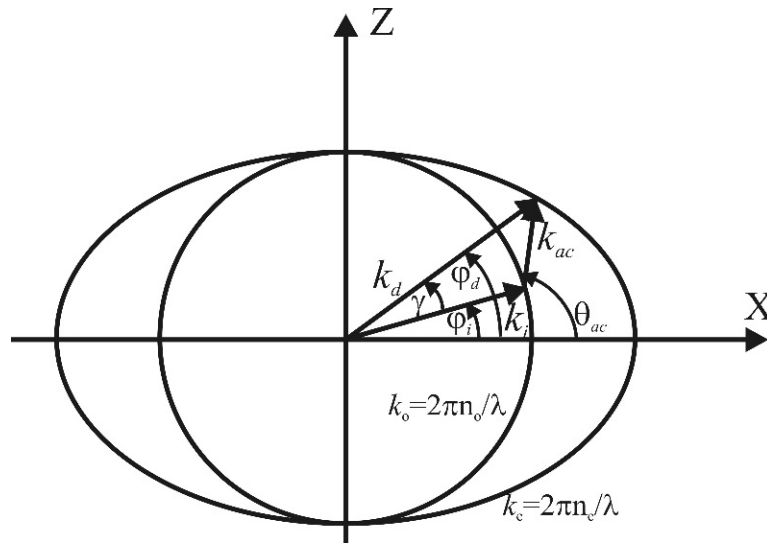


**Fig. 1.** Schematic vector diagram of anisotropic AO interactions in lead germanate crystals ( $\theta_{ac}$  is the angle between the X axis and the wavevector of AW;  $k_i$ ,  $k_d$ , and  $k_{ac}$  are the wavevectors of the incident and diffracted optical waves and AW, respectively).

for the incident optical wave and

$$n_e^2(\varphi_d) = \frac{n_o^2 n_e^2}{n_o^2 \cos^2 \varphi_d + n_e^2 \sin^2 \varphi_d} \tag{10}$$

for the diffracted wave.

The AW velocities can be obtained on the basis of a Christoffel equation:

$$v_{11}^{QL} = \sqrt{\frac{\cos^2 \theta_{ac}(C_{11} + C_{44}) + \sin^2 \theta_{ac}(C_{44} + C_{33}) + \sqrt{(\cos^2 \theta_{ac}(C_{11} - C_{44}) + \sin^2 \theta_{ac}(C_{44} - C_{33}))^2 + \sin^2 2\theta_{ac}(C_{13} + C_{44})^2}}{2\rho}}, \tag{11}$$

$$v_{12}^{QT_2} = \sqrt{\frac{0.5 \cos^2 \theta_{ac}(C_{11} - C_{12}) + \sin^2 \theta_{ac} C_{44}}{\rho}}, \tag{12}$$

$$v_{13}^{QT_1} = \sqrt{\frac{\cos^2 \theta_{ac}(C_{11} + C_{44}) + \sin^2 \theta_{ac}(C_{44} + C_{33}) - \sqrt{(\cos^2 \theta_{ac}(C_{11} - C_{44}) + \sin^2 \theta_{ac}(C_{44} - C_{33}))^2 + \sin^2 2\theta_{ac}(C_{13} + C_{44})^2}}{2\rho}}. \tag{13}$$

The angle of deviation from the purely longitudinal polarization state for the QL AW reads as

$$\zeta_2 = \theta_{ac} - 0.5 \arctan \frac{\sin 2\theta_{ac}(C_{13} + C_{44})}{(\cos^2 \theta_{ac}(C_{11} - C_{44}) + \sin^2 \theta_{ac}(C_{44} - C_{33}))}. \tag{14}$$

Then, one can write the relations for effective EO coefficients for six types of isotropic AO interactions with accounting that the coefficients  $p_{44}$ ,  $p_{16}$ , and  $p_{45}$  are negligibly small. For the first and second types of AO interaction with QL AW of incident ordinary and extraordinary optical waves, the relations for effective EO coefficients are as follows:

$$p_{eff}^{2(I)} = 0.5 [p_{12} \cos \theta_{ac} \cos \xi_2 + p_{13} \sin \theta_{ac} \sin \xi_2]^2 + 0.5 \chi_d^2 [p_{12} \cos \theta_{ac} \cos \xi_2 + p_{13} \sin \theta_{ac} \sin \xi_2]^2, \tag{15}$$

$$p_{eff}^{2(II)} = 0.5 \left\{ \begin{aligned} & [p_{11} \cos \theta_{ac} \cos \xi_2 + p_{13} \sin \theta_{ac} \sin \xi_2]^2 \cos^2(\theta_{ac} - \theta_B) \\ & + [p_{31} \cos \theta_{ac} \cos \xi_2 + p_{33} \sin \theta_{ac} \sin \xi_2]^2 \sin^2(\theta_{ac} - \theta_B) \end{aligned} \right\} \\ + 0.5 \chi_d^2 \left\{ \begin{aligned} & [p_{11} \cos \theta_{ac} \cos \xi_2 + p_{13} \sin \theta_{ac} \sin \xi_2]^2 \cos^2(\theta_{ac} - \theta_B) \\ & + [p_{31} \cos \theta_{ac} \cos \xi_2 + p_{33} \sin \theta_{ac} \sin \xi_2]^2 \sin^2(\theta_{ac} - \theta_B) \end{aligned} \right\}. \quad (16)$$

For the third and fourth types of AO interaction with QT<sub>1</sub> AW, which is polarized in the XZ plane, the respective relation can be written as:

$$p_{eff}^{2(III)} = 0.5 [p_{13} \sin \theta_{ac} \cos \xi_2 - p_{12} \cos \theta_{ac} \sin \xi_2]^2 \\ + 0.5 \chi_d^2 [p_{13} \sin \theta_{ac} \cos \xi_2 - p_{12} \cos \theta_{ac} \sin \xi_2]^2, \quad (17)$$

$$p_{eff}^{2(IV)} = 0.5 \left\{ \begin{aligned} & [p_{13} \sin \theta_{ac} \cos \xi_2 - p_{11} \cos \theta_{ac} \sin \xi_2]^2 \cos^2(\theta_{ac} - \theta_B) \\ & + [p_{33} \sin \theta_{ac} \cos \xi_2 - p_{31} \cos \theta_{ac} \sin \xi_2]^2 \sin^2(\theta_{ac} - \theta_B) \end{aligned} \right\} \\ + 0.5 \chi_d^2 \left\{ \begin{aligned} & [p_{13} \sin \theta_{ac} \cos \xi_2 - p_{11} \cos \theta_{ac} \sin \xi_2]^2 \cos^2(\theta_{ac} - \theta_B) \\ & + [p_{33} \sin \theta_{ac} \cos \xi_2 - p_{31} \cos \theta_{ac} \sin \xi_2]^2 \sin^2(\theta_{ac} - \theta_B) \end{aligned} \right\}. \quad (18)$$

The relations for effective EO coefficients for the fifth and sixth types of isotropic interactions with QT<sub>2</sub> AW, which is polarized parallel to the Y axis, have the view:

$$p_{eff}^{2(V)} = 0.5 \chi_i^2 \{ p_{66}^2 \cos^2 \theta_{ac} \cos^2(\theta_{ac} - \theta_B) \} \\ + 0.5 \chi_i^2 \chi_d^2 \{ p_{66}^2 \cos^2 \theta_{ac} \cos^2(\theta_{ac} - \theta_B) \}, \quad (19)$$

$$p_{eff}^{2(VI)} = 0.5 \chi_i^2 p_{66}^2 \cos^2 \theta_{ac} + 0.5 \chi_i^2 \chi_d^2 p_{66}^2 \cos^2 \theta_{ac}. \quad (20)$$

The relations for effective EO coefficients are as follows for the seventh, eighth, and nine types of anisotropic AO interaction with QL, QT<sub>1</sub>, and QT<sub>2</sub> AWs:

$$p_{eff}^{2(VII)} = \chi_i^2 \left\{ \begin{aligned} & (p_{11} \cos \theta_{ac} \cos \xi_2 + p_{13} \sin \theta_{ac} \sin \xi_2)^2 \cos^2(\theta_{ac} - \theta_B) \\ & + (p_{31} \cos \theta_{ac} \cos \xi_2 + p_{33} \sin \theta_{ac} \sin \xi_2)^2 \sin^2(\theta_{ac} - \theta_B) \end{aligned} \right\} \\ + \chi_d^2 \chi_i^2 \left\{ \begin{aligned} & (p_{11} \cos \theta_{ac} \cos \xi_2 + p_{13} \sin \theta_{ac} \sin \xi_2)^2 \cos^2(\theta_{ac} - \theta_B) \\ & + (p_{31} \cos \theta_{ac} \cos \xi_2 + p_{33} \sin \theta_{ac} \sin \xi_2)^2 \sin^2(\theta_{ac} - \theta_B) \end{aligned} \right\}, \quad (21)$$

$$p_{eff}^{2(VIII)} = \chi_i^2 \left\{ \begin{aligned} & (p_{13} \sin \theta_{ac} \cos \xi_2 - p_{11} \cos \theta_{ac} \sin \xi_2)^2 \cos^2(\theta_{ac} - \theta_B) \\ & + (p_{33} \sin \theta_{ac} \cos \xi_2 - p_{31} \cos \theta_{ac} \sin \xi_2)^2 \sin^2(\theta_{ac} - \theta_B) \end{aligned} \right\} \\ + \chi_d^2 \chi_i^2 \left\{ \begin{aligned} & (p_{13} \sin \theta_{ac} \cos \xi_2 - p_{11} \cos \theta_{ac} \sin \xi_2)^2 \cos^2(\theta_{ac} - \theta_B) \\ & + (p_{33} \sin \theta_{ac} \cos \xi_2 - p_{31} \cos \theta_{ac} \sin \xi_2)^2 \sin^2(\theta_{ac} - \theta_B) \end{aligned} \right\}, \quad (22)$$

$$p_{eff}^{2(IX)} = p_{66}^2 \cos^2 \theta_{ac}, \quad (23)$$

respectively.

As seen from Fig. 1, the direction of the AW vector changes when the angle  $\varphi_i$  does. For instance, we deal with a collinear AO diffraction whenever  $\gamma$  is equal to 0 or 180 deg. Then the three wave vectors, the wave vectors of the two optical waves and the AW, remain collinear. This kind of interaction cannot be accomplished when  $\varphi_i = 90$  or 270 deg, without accounting of circular birefringence since the linear birefringence is equal to zero along these

directions. The direction of the AW vector is uniquely determined by the angle  $\theta_{ac}$  between the AW vector and the  $X$  axis:

$$\theta_{ac} = \pi + \arctan \left[ \frac{\left( \frac{(n_o + A)(n_o + B)}{\sqrt{\cos^2 \varphi_d (n_o + B)^2 + \sin^2 \varphi_d (n_o + A)^2}} \right) \sin \varphi_d - \left( \frac{(n_o - A)(n_o - B)}{\sqrt{\cos^2 \varphi_i (n_o - B)^2 + \sin^2 \varphi_i (n_o - A)^2}} \right) \sin \varphi_i}{\left( \frac{(n_o + A)(n_o + B)}{\sqrt{\cos^2 \varphi_d (n_o + B)^2 + \sin^2 \varphi_d (n_o + A)^2}} \right) \cos \varphi_d - \left( \frac{(n_o - A)(n_o - B)}{\sqrt{\cos^2 \varphi_i (n_o - B)^2 + \sin^2 \varphi_i (n_o - A)^2}} \right) \cos \varphi_i} \right], \quad (24)$$

where  $A = g_{11}^2 / (2n_o(n_o^2 - n_e^2))$  and  $B = g_{33}^2 / (2(n_e^2 - n_o^2)n_o)$  (since  $\varphi_d = \varphi_i + \gamma$  the addition  $\pi$  at  $\gamma = 0$  should be omitted). The relations for the effective EO coefficients for XII – IX types of anisotropic diffraction have been obtained using the same procedure as it was described in our recent work [10].

### 3. Results and discussion

#### 3.1. Isotropic diffraction

The dependencies of effective EO coefficients and AO figures of merit on  $\theta_{ac}$  for  $\text{Pb}_5\text{Ge}_3\text{O}_{11}$  crystals for the first type of AO interaction at room temperature ( $T=298$  K) and the temperature close to the phase transition ( $T=448$  K) are presented in Fig. 2 as an example. It is seen that at  $\theta_{ac}=0$  deg, the effective EO coefficient and AO figure of merit exhibit peak-like dependencies. Notice that at  $\theta_{ac}=0$  deg, the incident and diffracted optical waves propagate close to the optical axis where the ellipticity of eigenwaves approach unity. At these conditions (see, e.g., Eq. (15)), the term that describes the contribution caused by the ellipticity reaches its maximal value. As one can see, the peaks are of the same magnitude for  $T=298$  K and 448 K. However, the full width at half maximum (FWHM) is different. The FWHM for  $T=298$  K is greater than for  $T=448$  K.

The FWHM of the peak of the AO figure of merit is the important parameter in the case of AO diffraction since it determinates the range of angles of incident and diffracted beam in which the enhancement of AO figure of merit due to the ellipticity of eigenwaves is possible. Let us remind that in our recent work [11], it has been shown that FWHM increases with increasing circular birefringence. The dependencies of half of FWHM of the peak of the AO figure of merit on angle  $\theta_{ac}$  for the I-st and II-nd types of AO interaction are presented in Fig. 3. It is seen that the AO figure of merit increases about three times when angle  $\theta_{ac}$  approaches zero. The peak value is almost the same in the maximum for all temperatures. At the same time, the FWHM increases when the temperature decreases from Curie's temperature to room one.

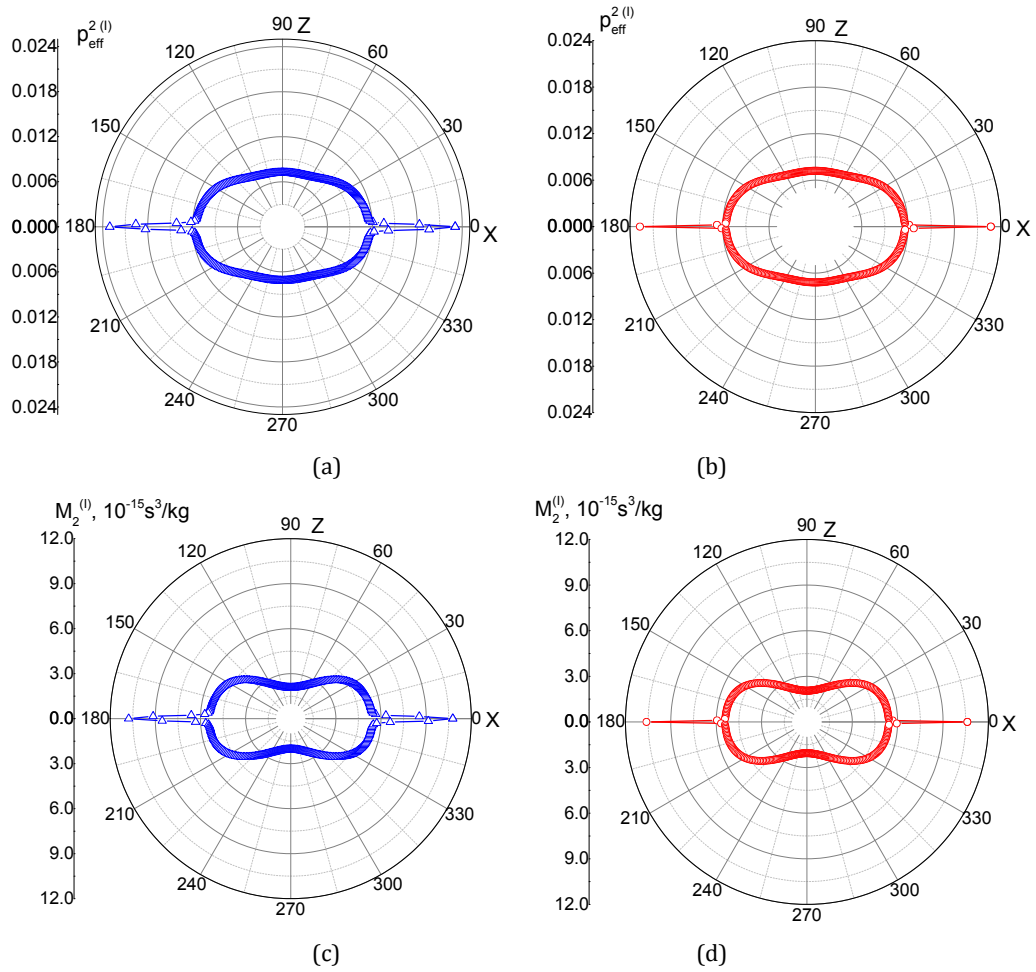


**Fig. 2.** Dependencies of effective EO coefficients (a, b) and AO figures of merit (c, d) on  $\theta_{ac}$  for  $\text{Pb}_5\text{Ge}_3\text{O}_{11}$  crystals for the first type of AO interaction at room temperature ( $T=298$  K) (a, c) and the temperature close to the phase transition ( $T=448$  K) (b, d).

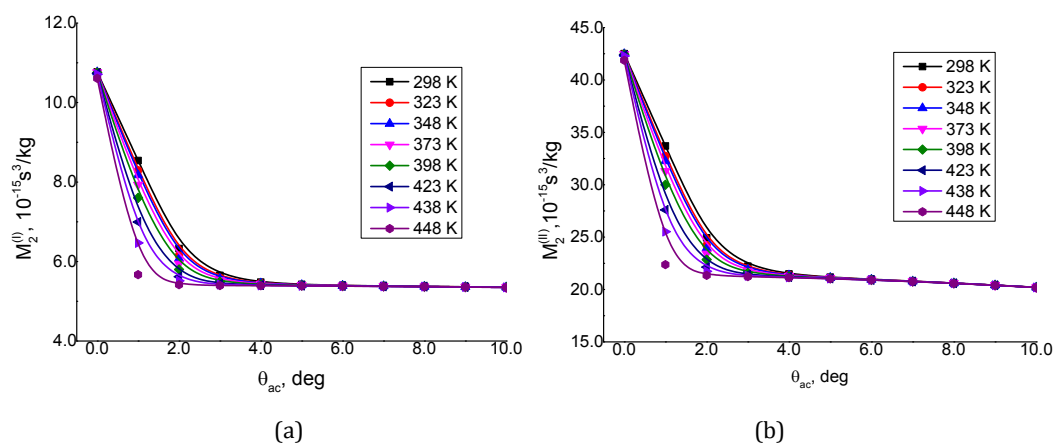


**Fig. 3.** The dependencies of half of FWHM of the peak of the AO figure of merit on angle  $\theta_{ac}$  for the I-st (a) and II-nd (b) types of AO interaction.

It should be noted that for the III and IV types of AO interaction, the peak of effective EO coefficient vanishes since at  $\theta_{ac} = 0$ , the non-orthogonality angle  $\xi_2 = 0$ , and as a result, both  $p_{eff}^{2(III)}$  and  $p_{eff}^{2(IV)}$  are equal to zero. As mentioned above, the value of spontaneous polarization corresponds to a certain temperature within the ferroelectric phase, while the spontaneous polarization can be recalculated to the electric field using Eq. (3). Therefore, let us analyze the dependencies of FWHM of the peak of the AO figure of merit on electric field.

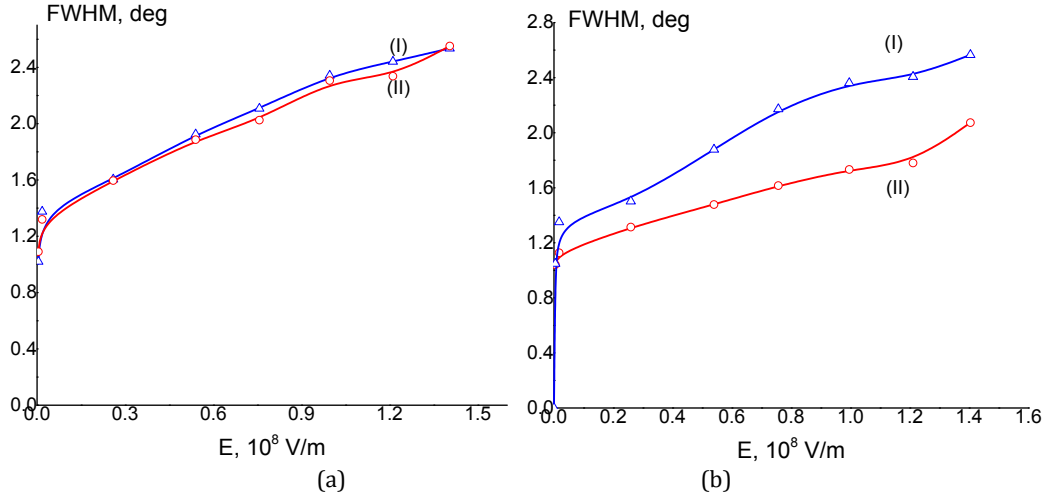


**Fig. 4.** The dependencies of FWHM of the peak of the AO figure of merit on the electric field for I - triangles and II - circles (a) and V - triangles and VI - circles (b) types of AO interactions.

As seen (Fig. 4), the FWHM of the peak of the AO figure of merit increases with the growth of the electric field and tends to saturation. The saturation starts from the value of the electric field of about  $2 \times 10^6$  V/m. The behavior of FWHMs in an electric field is similar to those that were revealed by us in a magnetic field due to the Faraday effect [11].

### 3.2. Anisotropic diffraction

As it is seen from Eqs. (21, 22) the relations for effective EO coefficients for the VII and VIII types of AO interaction with the QL and  $QT_1$  AWs, respectively, do not contain terms independent of eigenwaves' ellipticity. Therefore, without optical activity, the anisotropic AO interaction with these AWs cannot be accomplished. The electric field that causes the optical activity due to the electro-gyration leads to the appearance of the possibility of realization of AO diffraction of VII and VIII types. At the diffraction angle  $\gamma$  equal to 0 and 180 deg, one can observe the drop of the AO figure of merit (Fig. 5a). This drop appears because at these values of diffraction angles, one deals with the collinear type of interaction of so-called transmission and reflection types. At the same time, the case when  $\varphi_i$  is equal to 89 deg has been considered, i.e., the incident and diffracted waves propagate close to the optical axis where the collinear AO interaction cannot be realized except in the case of the presence of the circular birefringence. However, there is a lack of respective nonzero EO coefficients for the VII type of AO interaction to satisfy the conditions of collinear AO interaction with circularly polarized optical waves. It is seen that for the VII type of AO interaction, the maximum value of the AO figure of merit appears at a diffraction angle equal to 38.0 deg (Fig. 5b).



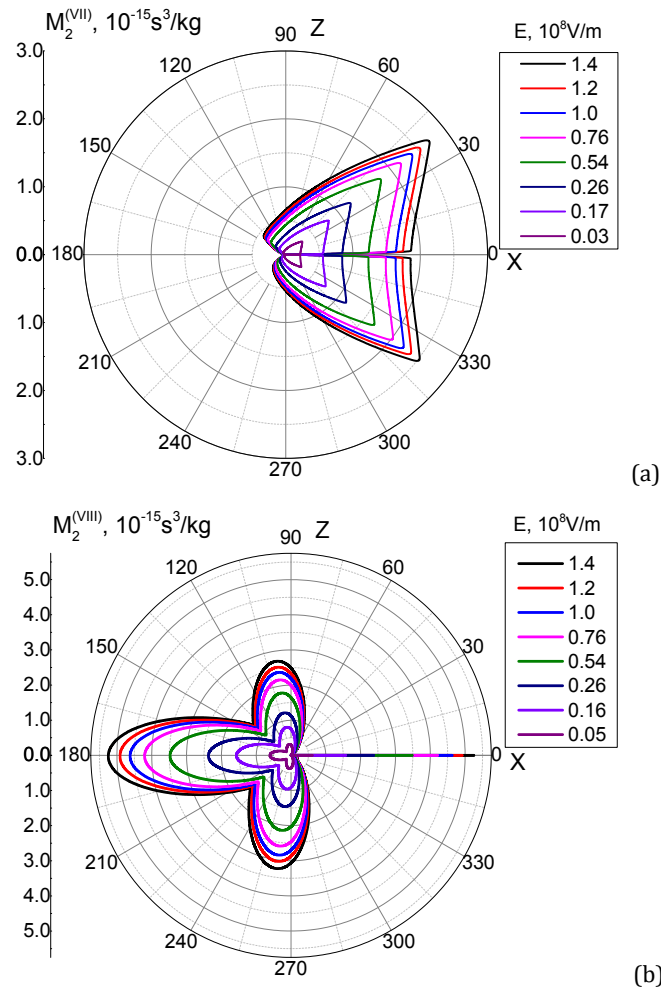


**Fig. 5.** The dependencies of the AO figure of merit on the diffraction angle  $\gamma$  for the VII (a) and VIII (b) types of AO interaction ( $\varphi_i=89$  deg).

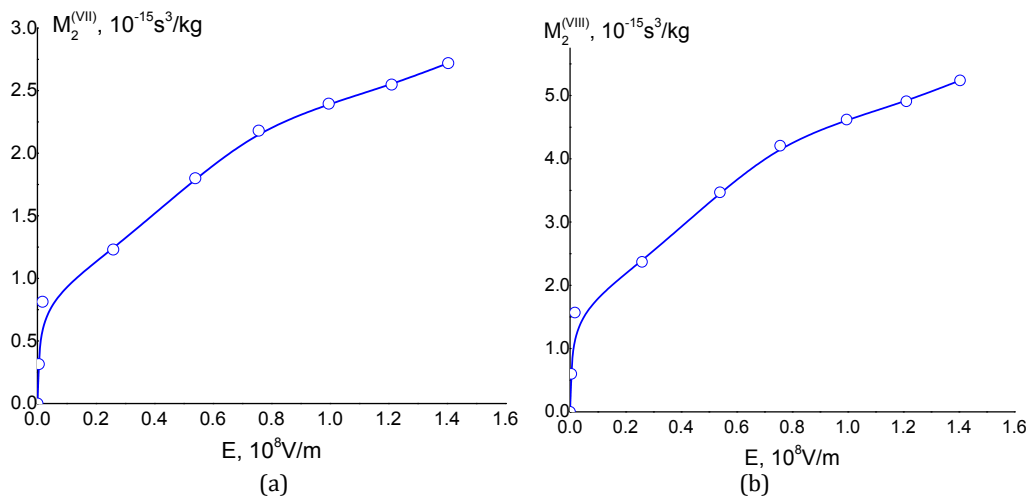


**Fig. 6.** The dependencies of the AO figure of merit on the electric field at VII (a) and VIII (b) types of AO interaction (for VII type of AO interaction  $\varphi_i=89.0$  deg,  $\gamma=38.0$  deg; for VIII type of AO interaction  $\varphi_i=89.0$  deg,  $\gamma=0.0$  deg (or  $180.0$  deg)).

At the VIII type of AO interaction, the maximum value of the AO figure of merit is reached for a diffraction angle equal to 0 and 180 deg, i.e., for the collinear type of diffraction.

The increasing electric field induces the expansion of the AO figure of merit surfaces (Figs. 5,6). The dependencies of the AO figure of merit taken for diffraction angles at which it reaches the maximal values are presented in Fig. 6. It is seen that for both types of AO interaction, these dependencies are similar – the increasing of electric field strength leads to saturation-like dependence of AO figure of merit. It is interesting to notice that at the VIII type of interaction, the AO figure of merit for collinear diffraction is quite high, i.e.,  $\sim 5 \times 10^{-15} \text{s}^3/\text{kg}$  whenever the electric field strength is of  $\sim 10^8 \text{V/m}$ .

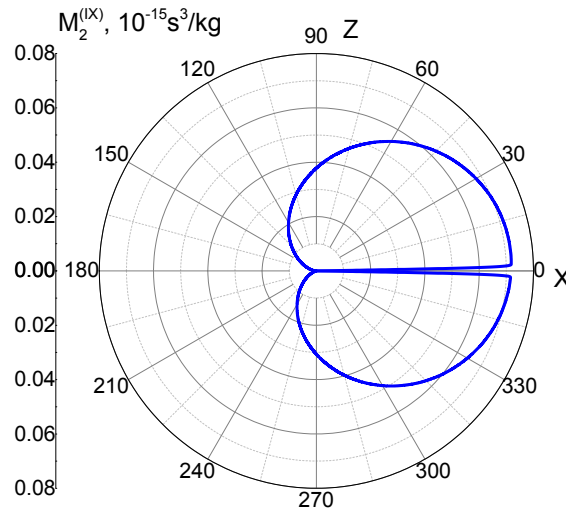


**Fig. 7.** Dependence of AO figure of merit on the diffraction angle at the IX type of AO interaction ( $\varphi_i=89$  deg)

The effective EO coefficient for IX type of AO interaction with pure transverse AW QT<sub>2</sub> is determined solely by the component of EO tensor  $p_{66}$  (see Eq. (23)). Moreover, the ellipticity of the eigenwaves does not affect the effective EO coefficient. The dependence of the AO figure of merit on the diffraction angle for the IX type of AO interaction is presented in Fig. 7. At the diffraction angle  $\gamma$  equal to 0 and 180 deg, one can observe the drop of the AO figure of merit (Fig. 7). This drop appears because at these values of diffraction angles, one deals with the collinear type of interaction, which cannot be realized since there are no respective EO coefficients.

#### 4. Conclusions

In the present work, we have shown for the first time that the electric field can enhance the AO figure of merit and, hence, the AO efficiency due to the induced ellipticity of eigenwaves through the electro-gyration effect. The analysis was made using the example of proper ferroelectric Pb<sub>5</sub>Ge<sub>3</sub>O<sub>11</sub> crystals, for which the spontaneous polarization was recalculated to the electric field. It has been shown that for the isotropic types of interaction, the strength of the electric field results in the broadening of the FWHM of the peak of the AO figure of merit and almost does not affect the maximal value of this peak. At the increasing of electric field strength value, the FWHM of the peak of the AO figure of merit manifests saturation-like dependence. For anisotropic types of diffraction, the behavior of the AO figure of merit

differs from those for isotropic types of diffraction. The peak of the AO figure of merit is not observed. But with increasing the electric field strength, the surface of the AO figure of merit is expanded.

**Acknowledgement.** The authors acknowledge the Ministry of Education and Science of Ukraine for financial support of this study (project # 0123U101781).

## References

1. Magdich, L. N. (1989). *Acoustooptic devices and their applications*. CRC Press.
2. Mys, O., Krupych, O., & Vlokh, R. (2016). Anisotropy of an acousto-optic figure of merit for  $\text{NaBi}(\text{MoO}_4)_2$  crystals. *Applied Optics*, 55(28), 7941-7955.
3. Mys, O., Adamenko, D., Krupych, O., & Vlokh, R. (2018). Effect of deviation from purely transverse and longitudinal polarization states of acoustic waves on the anisotropy of acousto-optic figure of merit: the case of  $\text{Ti}_3\text{As}_4$  crystals. *Applied Optics*, 57(28), 8320-8330.
4. Mys, O., Krupych, O., Martynyuk-Lototska, I., Orykhivskiy, I., Kostyrko, M., & Vlokh, R. (2021). Types of acousto-optic interactions between acoustic and circularly polarized optical waves: case of  $\text{Pb}_5\text{Ge}_3\text{O}_{11}$  crystals. *Applied Optics*, 60(10), 2846-2853.
5. Andrushchak, A. S., Chernyshivsky, E. M., Gotra, Z. Y., Kaidan, M. V., Kityk, A. V., Andrushchak, N. A., Maksymyuk, T. A., Mytsyk, B. G. & Schranz, W. (2010). Spatial anisotropy of the acousto-optical efficiency in lithium niobate crystals. *Journal of Applied Physics*, 108(10).
6. Buryy, O., Andrushchak, N., Ratych, A., Demyanyshyn N., Mytsyk B., and Andrushchak A. (2017). Global maxima for the acousto-optic effect in  $\text{SrB}_4\text{O}_7$  crystals. *Applied Optics*, 56(7), 1839-1845.
7. Zyuryukin, Y. A., Zavarin, S. V., & Yulaev, A. N. (2009). Characteristic features of wideband anisotropic light diffraction in lithium-niobate crystal by a longitudinal acoustic wave. *Optics and Spectroscopy*, 107, 152-156.
8. Mys, O., Kostyrko, M., Adamenko, D., Martynyuk-Lototska, I., Skab, I., & Vlokh, R. (2022). Effect of ellipticity of optical eigenwaves on the enhancement of efficiency of acousto-optic Bragg diffraction. A case of optically active  $\text{Pb}_5\text{Ge}_3\text{O}_{11}$  crystals. *AIP Advances*, 12(5).
9. Mys, O., Adamenko, D., & Vlokh, R. (2023). Enhancement of acousto-optic diffraction efficiency in  $\text{SiO}_2$  crystals due to ellipticity of optical eigenwaves: isotropic acousto-optic interaction. *Ukrainian Journal of Physical Optics*, 24(2), 124-134.
10. Mys, O., Adamenko, D., & Vlokh, R. (2023). Increase in the acousto-optic figure of merit in  $\text{SiO}_2$  crystals due to optical activity. Anisotropic acousto-optic interactions. *Ukrainian Journal of Physical Optics*, 24(3), 262-275.
11. Mys, O., Adamenko, D., & Vlokh, R. (2023). Influence of Faraday elliptical birefringence on the acousto-optic diffraction efficiency: a case of isotropic interaction with quasi-longitudinal acoustic waves in  $\text{KH}_2\text{PO}_4$  crystals. Errata. *Ukrainian Journal of Physical Optics*, 24(4), 04087-04087.
12. Iwasaki, H., Miyazawa, S., Koizumi, H., Sugii, K., & Niizeki, N. (1972). Ferroelectric and optical properties of  $\text{Pb}_5\text{Ge}_3\text{O}_{11}$  and its isomorphous compound  $\text{Pb}_5\text{Ge}_2\text{SiO}_{11}$ . *Journal of Applied Physics*, 43(12), 4907-4915.
13. Dougherty, J. P., Sawaguchi, E., & Cross, L. E. (1972). Ferroelectric Optical Rotation Domains in Single-Crystal  $\text{Pb}_5\text{Ge}_3\text{O}_{11}$ . *Applied Physics Letters*, 20(9), 364-365.
14. Vlokh, O., Kushnir, O., & Shopa, Y. (1992). Gyrotropic properties of  $\text{Pb}_5\text{Ge}_3\text{O}_{11}$  ferroelectric crystals. *Ferroelectrics*, 126(1), 97-102.
15. Adamenko, D. I., Vlokh, R. O. (2022). Critical exponents of the order parameter of diffuse ferroelectric phase transitions in the solid solutions based on lead germanate: studies of optical rotation. *Condensed Matter Physics*, 25(4), 43703.
16. Iwasaki, H., & Sugii, K. (1971). Optical activity of ferroelectric  $5\text{PbO} \cdot 3\text{GeO}_2$  single crystals. *Applied Physics Letters*, 19(4), 92-93.
17. Martynyuk-Lototska, I., Mys, O., Dudok, T., Mytsyk, B., Demyanyshyn, N., Kostyrko, M., Adamenko, D., Trubitsyn, M. & Vlokh, R. (2020). Experimental determination of full matrices of the piezo-optic and elasto-optic coefficients for  $\text{Pb}_5\text{Ge}_3\text{O}_{11}$  crystals. *Applied Optics*, 59(22), 6717-6723.
18. Konstantinova, A. F., Grechushnikov, B. N., Bokut, B. V., & Valyashko, E. G. (1995). Opticheskie svoistva kristallov (Optical Properties of Crystals). *Minsk: Navuka Tekhnika*.

Mys O., Adamenko D., Vlokh R. (2024). Enhancement of the Efficiency of Acousto-Optic Diffraction Due to the Ellipticity of Eigen Optical Waves, Caused by the Electro-Gyration Effect in Lead Germanate Crystals. *Ukrainian Journal of Physical Optics*, 25(3), 03001 – 03012. doi: 10.3116/16091833/Ukr.J.Phys.Opt.2024.03001

**Анотація.** В роботі вперше показано, що електричне поле може підвищити коефіцієнт акустооптичної (АО) якості завдяки індукованій еліптичності власних хвиль через ефект електрогірації. У результаті аналізу виявлено, що для ізотропних типів взаємодії напруженість електричного поля призводить до розширення ширини на піввисоті (ШПВ) піку коефіцієнта АО якості, тоді як вона майже не впливає на

максимальне значення цього піку. ШПВ піку коефіцієнта АО якості прямує до насичення зі збільшенням напруженості електричного поля. Для анізотропних типів дифракції пік коефіцієнта АО якості не спостерігається, але зі збільшенням напруженості електричного поля поверхня цього коефіцієнта розширюється.

**Ключові слова:** акустооптична дифракція, коефіцієнт акустооптичної якості, ефективний пружнооптичний коефіцієнт, електрогірація, оптична активність, еліптичність власних оптичних хвиль